The American Journal of Pathology, Vol. 185, No. 1, January 2015

The American Journal of
PATHOLOGY
ajp.amjpathol.org

CARDIOVASCULAR, PULMONARY, AND RENAL PATHOLOGY

Activation of the Wnt/Planar Cell Polarity Pathway Is Required for Pericyte Recruitment during Pulmonary Angiogenesis

Ke Yuan,[*†] Mark E. Orcholski,[*†] Cristina Panaroni,[‡] Eric M. Shuffle,[*†] Ngan F. Huang,[†§¶] Xinguo Jiang,[†§] Wen Tian,[†§] Eszter K. Vladar,[‖] Lingli Wang,[**] Mark R. Nicolls,[†§] Joy Y. Wu,[‡] and Vinicio A. de Jesus Perez[*†]

From the Divisions of Pulmonary and Critical Care Medicine and Endocrinology, Gerontology & Metabolism,[‡] the Stanford Cardiovascular Institute,[†] the VA Palo Alto Health Care System,[§] and the Department of Cardiothoracic Surgery,[¶] Stanford University, Stanford; and the Department of Pathology,[‖] Vera Moulton Wall Center for Pulmonary Vascular Disease, and Department of Pediatrics,[**] Stanford University School of Medicine, Stanford, California*

Accepted for publication September 3, 2014.

Address correspondence to Vinicio A. de Jesus Perez, M.D., Division of Pulmonary and Critical Care Medicine, Stanford University Medical Center, 300 Pasteur Dr., Grant S140B, Stanford, CA 94305. E-mail: vdejesus@stanford.edu.

Pericytes are perivascular cells localized to capillaries that promote vessel maturation, and their absence can contribute to vessel loss. Whether impaired endothelial—pericyte interaction contributes to small vessel loss in pulmonary arterial hypertension (PAH) is unclear. Using 3G5-specific, immunoglobulin G—coated magnetic beads, we isolated pericytes from the lungs of healthy subjects and PAH patients, followed by lineage validation. PAH pericytes seeded with healthy pulmonary microvascular endothelial cells failed to associate with endothelial tubes, resulting in smaller vascular networks compared to those with healthy pericytes. After the demonstration of abnormal polarization toward endothelium via live-imaging and wound-healing studies, we screened PAH pericytes for abnormalities in the Wnt/planar cell polarity (PCP) pathway, which has been shown to regulate cell motility and polarity in the pulmonary vasculature. PAH pericytes had reduced expression of frizzled 7 (*Fzd7*) and *cdc42*, genes crucial for Wnt/PCP activation. With simultaneous knockdown of Fzd7 and cdc42 in healthy pericytes *in vitro* and in a murine model of angiogenesis, motility and polarization toward pulmonary microvascular endothelial cells were reduced, whereas with restoration of both genes in PAH pericytes, endothelial—pericyte association was improved, with larger vascular networks. These studies suggest that the motility and polarity of pericytes during pulmonary angiogenesis are regulated by Wnt/PCP activation, which can be targeted to prevent vessel loss in PAH. *(Am J Pathol 2015, 185: 69—84; http://dx.doi.org/10.1016/j.ajpath.2014.09.013)*

Pericytes are highly specialized vascular cells that directly interact with endothelial cells (ECs) to provide mural support and to help promote small vessel maturation and survival.[1–3] The definition of a mature pericyte is very controversial, but the currently accepted definition describes cells embedded within the vascular basement membrane of blood microvessels making specific focal contacts with endothelium, that is, capillaries, postcapillary venules, and terminal arterioles.[3] Pericytes closely interact with ECs through both paracrine and juxtacrine mechanisms.[4] Loss or dysfunction of pericytes is involved in multiple pathologies, such as Alzheimer disease, hypertension, diabetic retinopathy, and tumor angiogenesis.[5–8] To date, most studies have centered on elucidating the contribution of pericytes to systemic microvessel, but very little is known about their role in the pulmonary circulation.

Lung pericytes can be found at the level of small precapillary arteries (<30 μm), capillaries (approximately 10 μm) and postcapillary venules, where they provide mural support and regulate vasomotor tone.[9] Whereas larger

Supported by postdoctoral fellowships from the American Heart Association (13POST17120040 to K.Y.), the Stanford Translational Research Seed Grant School of Medicine (K.Y.), NIH grant K08 HL105884-01, a Harold Amos Career Development Award, an American Lung Association Biomedical Research Award, the Stanford Translational Research and Applied Medicine Program, and the Stanford Cardiovascular Institute (V.A.d.J.P.).

Disclosures: None declared.

http://dx.doi.org/10.1016/j.ajpath.2014.09.013

(>50 μm) pulmonary arteries (PA) are fully enveloped by multiple layers of smooth muscle cells (PASMCs), precapillary arteries are only partially enveloped by pericytes.[9] This structural arrangement is important for lung function as the pulmonary circulation is designed to be a low-pressure, high-compliance system capable of accommodating the entire cardiac output for optimal oxygenation and rapid delivery to the left ventricle for systemic distribution. However, when these precapillary arteries become muscularized, pulmonary vascular resistance and impedance increase, resulting in pulmonary arterial hypertension (PAH), a life-threatening disorder associated with a progressive rise in pulmonary pressures resulting from: i) loss of and/or impaired regeneration of small peripheral pulmonary arteries, ii) occlusion of larger proximal pulmonary arteries due to uncontrolled proliferation of smooth muscle cells, and iii) deposition of extracellular matrix.[10] Efforts to elucidate the mechanisms related to small vessel loss in PAH have centered mostly on pulmonary ECs, but little is known about the contribution of pulmonary pericytes to PAH pathobiology. Recently, a study looked at pericyte distribution in the pulmonary circulation of PAH patients and reported increased pericyte numbers in close proximity to pulmonary microvessels, along with a pro-proliferative and promigratory phenotype when the cells were purified and cultured *in vitro*.[11] Although these observations seem to support a potential contribution of these cells to PAH pathology, it is still unclear whether the ability of pericytes to establish functional cell−cell contacts with ECs in pulmonary microvessels is also adversely affected in PAH. Given the role of pericytes in promoting the growth and maturation of microvessels, we predicted that failure of pericytes to associate with ECs in PAH could contribute to small vessel loss by preventing proper vascular growth, structural stability, and survival.

Here, we demonstrate for the first time that PAH pericytes purified from the lung of PAH patients using a unique recombinant anti−3G5-immunoglobulin (Ig)G failed to properly associate with endothelial tubes *in vitro,* resulting in smaller vascular networks and thinner endothelial tubes. We show that this is due to an intrinsic defect in cell motility and polarization that impairs the ability of PAH pericytes to migrate toward the vascular tubes, resulting in a significantly lower number of endothelial-pericyte interactions. We further show that these defects correlate with reduced activity of the Wnt/planar cell polarity (PCP), a pathway known to be crucial for the control for cell motility and polarity, resulting from reduced expression of frizzled 7 (Fzd7) and cdc42, key components of this signaling pathway. Taken together, our study provides the first evidence that PAH pericytes contribute to small vessel loss in PAH and that therapeutic strategies capable of restoring Wnt/PCP activity in these cells could help to prevent loss and/or facilitate small vessel regeneration in patients afflicted with this devastating disease.

Materials and Methods

Cell Culture

Control pulmonary microvascular ECs (PMVECs; PromoKine catalog number C-12282; PromoCell GmbH, Heidelberg, Germany) were grown in EC media (PromoKine catalog number C-22120; PromoCell GmbH) with growth supplements and used between passages 4 to 8.

Generation of 3G5 IgG1 Antibody

3G5 (ATCC CRL-1814) hybridoma cells were cultured in 1× Dulbecco's modified Eagle's medium with 10% fetal bovine serum (FBS). Culture medium was collected and concentrated by centrifugal filter Amicon Ultra-15 (Millipore Corporation, Billerica, MA). The 3G5 IgM was isolated using the IgM Purification Kit (Pierce Biotechnology, Inc., Rockford, IL), and its concentration was later determined by the Lowry method. IgM isotype switch to mouse IgG was performed and validated by LakePharma LLC (San Carlos, CA). Briefly, variable regions of 3G5 IgM antibody heavy and light chains were sequenced. Then, cDNAs of IgM heavy and light chains were constructed and cloned into pcDNA3 containing murine IgG light and heavy chain constant regions, respectively. Both plasmids were simultaneously transfected into HEK293 cells, which produced and released the recombinant 3G5 IgG antibody into the medium. The 3G5 IgG antibody was then purified using a commercial IgG purification kit.

Pericyte Isolation and Culture

Lung tissues from PAH and control patients were provided by the Pulmonary Hypertension Breakthrough Initiative, which is funded by the Cardiovascular Medical Research And Education Fund. The day before the pericyte isolation, 40 μL of M280 sheep anti-mouse IgG Dynabeads (11201D; Invitrogen Life Technologies Corporation, Carlsbad, CA) were incubated with 10 μg of 3G5 IgG overnight. The next day, fresh lung tissue was washed with 1× Hanks' balanced salt solution twice to remove medium. Then, tissue was minced and digested in a solution containing collagenase (Sigma-Aldrich, St. Louis, MO), dispase, and DNase I for 15 to 30 minutes at 37°C on an orbital shaker. An equivalent amount of cold pericyte medium (ScienCell Research Laboratories, Carlsbad, CA) containing 2% FBS was added immediately after digestion. The suspension was passed through a BD Falcon 100-μm mesh filter (BD Biosciences, San Jose, CA) to remove debris or undigested fibrous tissue. The cell pellet was resuspended in 1 mL 1× PBS containing 0.2% FBS and 40 μL of 3G5 IgG−coated magnetic beads and gently rotated at 4°C for 45 minutes. Beads were then washed five times with 1× PBS and seeded in gelatin-coated cell-culture plates with pericyte medium. Fresh medium was replaced every other day to promote pericyte attachment and propagation, which occurred after days 5 to 7. The clinical and

hemodynamic data from healthy donors and PAH patients who served as the sources of the pericytes are listed in Table 1.

Fluorescence-Activated Cell Sorting

Pericytes within passages 4 to 5 collected as described in *Pericyte Isolation and Culture* were serially propagated in complete pericyte media on gelatin-coated tissue culture plates for fluorescence-activated cell sorting. Immunophenotyping of cell surface molecules was performed by labeling cells with directly conjugated antibodies: NG-2-PE (FAB2585P; R&D Systems Inc., Minneapolis, MN), thymus cell antigen 1 (catalog number 562685; BD Biosciences), CD146-PE-Cy7 (catalog number 562135; BD Biosciences), platelet-derived growth factor receptor (PDGFR) β−PerCPC Y5.5 (catalog number 562714; BD Biosciences), CD31 PerCP-eFlow 710 (catalog number 46-0319-41; eBioscience, Inc., San Diego, CA), CD45-APC CY7 (catalog number 47-0459-41; eBioscience, Inc.), and 3G5 IgG. For assessing intracellular protein expression, cells were fixed and permeabilized with Cytofix/Cytoperm Plus (BD Biosciences) and incubated with the primary antibodies: α-smooth muscle actin (SMA)−fluorescein isothiocyanate (ab8211; Abcam plc, Cambridge, UK), calponin (ab700; Abcam plc), smooth muscle 22-α (SM22α; ab10135; Abcam plc), and smooth muscle myosin heavy chain (IC4470A; R&D Systems Inc.). At least 10,000 events were acquired for each sample on LSR II (BD Biosciences) and analyzed using FlowJo (Tree Star Inc., Ashland, OR). ECs, human brain pericytes (number 1200; ScienCell Research Laboratories), pulmonary arterial smooth muscle cells (number 3110; ScienCell Research Laboratories), and human blood mononuclear cells from buffy coat were analyzed in parallel as positive controls. Isotype controls were used as negative controls.

Immunofluorescence Staining

Around 1×10^4 cells were seeded on four-well EZ slides (Millipore Corporation) on the day before the staining. Next, cells were fixed for 15 minutes in 4% paraformaldehyde, followed by three washes with PBS. Cells were then permeabilized with ice-cold 1× PBS containing 0.1% Triton X-100 and goat serum for 1 hour, followed by overnight incubation with primary antibodies at 4°C, washed in 1× PBS, and incubated with Alexa Fluor 594

Table 1 Clinical Characteristics of Patient Samples

Patient type	Patient no.	Age, years	Sex	Etiology	6MWD (m)	Therapies	Hemodynamics	
							mPAP, mm Hg	PVR, WU
PAH	1	35	M	APAH-congenital systemic to pulmonary shunt-ASD	430	Sildenafil, bosentan	75	NA
	2	37	M	FPAH	309	Sildenafil, sitaxsentan, ambrisentan, epoprostenol, imatinib	77	14.22
	3	53	F	APAH-collagen vascular disease/ systemic lupus erythematous	400	Sildenafil, tadalafil, ambrisentan	58	19.34
	4	54	F	APAH-scleroderma	419	Sildenafil, ambrisentan, epoprostenol	NA	8.23
	5	13	F	APAH-congenital (s/p PDA ligation)	166	Sildenafil, bosentan, treprostinil	100	39
	6	14	F	IPAH	440	Tadalafil, ambrisentan, treprostinil	86	NA
	7	42	F	APAH-drugs and toxins-amphetamine	NA	Tadalafil, ambrisentan, treprostinil	52	NA
	8	7	F	IPAH	422.5	Sildenafil, ambrisentan, bosentan, iloprost, treprostinil	88	17.62
	9	28	M	IPAH	166.1	NA	77	NA
Failed Donor	1	26	M	Gunshot wound to the head				
	2	36	F	Subarachnoid hemorrhage				
	3	25	M	Cerebrovascular/stroke, intracranial hemorrhage				
	4	26	M	Drug intoxication/anoxia				
	5	60	F	Intracranial hemorrhage				
	6	30	M	Head trauma due to MVC				
	7	34	F	NA				
	8	49	F	Intracranial hemorrhage				
	9	57	F	Anoxia				

F, female; M, male; 6MWD, 6-minute walking distance; APAH, associated pulmonary arterial hypertension; ASD, atrial septal defect; FPAH, familial pulmonary arterial hypertension; IPAH, idiopathic pulmonary arterial hypertension; mPAP, mean pulmonary arterial pressure; MVC, motor vehicle crash; NA, not available; PDA, patent ductus arteriosus; PVR, pulmonary vascular resistance; WU, Wood units.

goat anti-mouse antibody and/or Alexa Fluor 488 goat anti-rabbit (A11008; Invitrogen) accordingly for 1 hour at room temperature. Slides were mounted with Prolong Gold antifade solution containing DAPI (Invitrogen).

Matrigel Co-Culture Tube-Formation Assay

Matrigel (Basement Membrane Extract, Trevigen, Gaithersburg, MD) was thawed on ice overnight and dispersed on 96-well plates (55 μL per plate) and allowed to polymerize for 30 minutes at 37°C. PMVECs and pericytes were stained with the cell membrane dyes PKH67 (MINI67; Sigma-Aldrich) and PKH26 (MINI26; Sigma-Aldrich), respectively, following the manufacturer's protocol. Around 5000 PMVECs were mixed with 1000 pericytes in 100 μL 2% FBS pericyte medium and then loaded on each Matrigel-coated well. After 4 hours, images were obtained and assessed by using a DMRB II fluorescence microscope (Leica Microsystems Inc., Buffalo Grove, IL). Total numbers of tubes, branching points, and loops were quantified using Wimasis software (Wimasis GmbH, Munich, Germany). Mean values for pericyte coverage of endothelial tubes were obtained from three independent experiments.

Boyden Chamber Assay

Before the experiment, cells were synchronized in starvation media (0.1% FBS in pericyte media) for 48 hours. To evaluate cell migration, single-cell suspensions of 2×10^4 cells were plated in triplicate into 24-well, 8 μm—pore invasion chambers (3097; Becton, Dickinson, and Company, Franklin Lakes, NJ) according to the manufacturer's instructions. Translocated cells were quantified after 6 hours by hematoxylin and eosin staining. The mean number of cells in four 20× random fields was used for analysis.

Wound-Healing Co-Culture Assay

Cell-culture plates with inserts (catalog number 81176) were purchased from ibidi GmbH (Munich, Germany). Around 1.5×10^4 cells (PMVECs and pericytes) were seeded into either side of the inserts. Cells were synchronized using starvation media for 16 hours before removal of the inserts. Serial images of the gap between PMVECs and pericytes were taken over a period of 6 hours. Cell migration rate and orientation were calculated by comparing cells at 0 and 6 hours. Pericentrin (1:1000; ab4448; Abcam plc) and phalloidin-labeled F-actin (1:50; Invitrogen) were used to stain the microtubule-organizing center (MTOC) and actin filaments, respectively.

TaqMan Quantitative PCR

Quantitation of mRNA expression was determined by real-time quantitative RT-PCR (Applied Biosystems Inc., Foster City, CA) following the manufacturer's protocol. Briefly, 25 ng of mRNA (RNeasy Mini Kit, Qiagen, Germantown, MD) was used for each reaction. The PCR reaction mixture was denatured at 95°C for 15 minutes and then run for 40 cycles (94°C for 15 seconds, 55°C for 30 seconds, and 70°C for 30 seconds). Melting curve analysis was run at the same time to rule out nonspecific reactions or contamination. Glyceraldehyde-3-phosphate dehydrogenase was used for normalization. Agarose gel electrophoresis, using 1% gels, was used for verification of uncertain results. All quantitative PCR was run in triplicate. The difference in mRNA expression was determined by ΔΔCT. The reverse-transcription kit was purchased from Fermentas (Vilnius, Lithuania) and TaqMan PCR primer sets were purchased from Life Technologies.

Western Immunoblot Analysis

Cells were washed three times with ice-cold 1× PBS, and lysates were prepared by adding boiling lysis buffer (1× radioimmunoprecipitation assay buffer and 1 mmol/L phenylmethylsulfonyl fluoride), scraping into a 1.5-mL microcentrifuge tube, and boiling for 10 minutes before centrifugation. Supernatants were transferred to fresh microcentrifuge tubes and stored at −80°C. The protein concentration was determined by the Lowry assay (Bio-Rad Laboratories S.r.l., Segrate, Italy). Equal amounts of protein were loaded onto each lane of a 4% to 12% Bis- Tris gel (Life Technologies Corporation) and subjected to SDS-PAGE electrophoresis under reducing conditions. After blot analysis, polyvinylidene difluoride membranes were blocked for 1 hour in blocking buffer (5% milk powder in 0.1% PBS/Tween20) and incubated with primary antibodies for Fzd7 (ab64636; Abcam plc) and cdc42 (07-1466; Millipore Corporation) overnight at 4°C. Horseradish peroxidase conjugated secondary antibodies were visualized by Amersham ECL (GE Healthcare Bio-Sciences, Pittsburgh, PA). Signal normalization was performed with a mouse monoclonal antibody against α-tubulin (Sigma-Aldrich).

RNA Interference

To achieve gene knockdown, 2 μmol/L siRNA of Fzd7 (catalog number M-003671-02-0005; Thermo Fisher Scientific Inc., Rockford, IL) and/or 2 μmol/L siRNA of cdc42 (catalog number M-005057-01-0005; Thermo Fisher Scientific Inc.) or nontargeting siRNA control (catalog number D-001810-10-05; Thermo Fisher Scientific Inc.) was transfected into healthy pericytes. Knockdown efficiency was evaluated 72 hours after electroporation by measuring Fzd7 or total cdc42 protein levels in cell lysates via Western immunoblot analysis. Transfection was performed using an Amaxa Nucleofector II (program U-25) with the Basic Smooth Muscle Cell Nucleofector kit (Lonza, Basel, Switzerland). All Matrigel or wound-healing experiments were performed 72 hours after electroporation.

Plasmids

PAH pericytes were co-transfected with 1 μg of pCMV6-AC-Fzd7-GFP (RG204167; OriGene Technologies, Inc., Rockville, MD) and 1 μg of pCMV6-AC-cdc42-GFP

(RG214076; OriGene Technologies, Inc.) in a transfection device (Nucleofector II Program U-052; Lonza) using the basic SMC Nucleofector kit (Lonza). The empty pCMV6-AC-GFP vector (PS100010; OriGene Technologies, Inc.) served as a negative control. Cells were incubated with 200 μg/mL neomycin for antibiotic selection and were plated in Matrigel 48 hours later.

Active RhoA/Rac1/cdc42 Pull-Down Assays

Pericytes were cultured in pericytes medium (number 1201; ScienCell Research Laboratories) and in a 100-mm Petri dish until 80% confluence was reached. After cells were starved by 0.2% FBS medium for 24 hours, they were washed three times with ice-cold 1× PBS. Cell lysates were prepared by adding 500 μL of ice-cold magnesium lysis buffer (10 mmol/L Tris-HCl, 1.0% SDS, 0.2 mmol/L phenylmethylsulfonyl fluoride, and protease and phosphatase inhibitor cocktails I and II; Millipore Corporation) to the cells and scraping into a 1.5-mL microcentrifuge tube on ice before cold centrifugation at 14,000 × *g* for 10 minutes. Supernatants were transferred to fresh microcentrifuge tubes and stored at −80°C. Active forms of Rho protein A (RhoA) or Ras-related C3 botulinum toxin substrate 1 (Rac1) were precipitated using glutathione beads containing rhotekin or p21-activated kinase 1, respectively, according to the manufacturer's protocol (Millipore Corporation). In brief, lysates were incubated with slurry containing the glutathione beads for 1 hour at 4°C with constant rotation. At the end of this period, beads were precipitated by centrifuging lysates at 14,000 × *g* for 20 seconds. After washing three times with ice-cold buffer, beads were resuspended in Laemmli buffer, boiled, and subjected to Western immunoblot analysis.

Matrigel Plug Angiogenesis Assay in SCID Mice

Animal experiments were approved by Stanford University's institutional review board and followed the guidelines of the American Physiological Society. Matrigel plugs containing PMVECs alone or with pericytes were prepared as described previously.[12] Briefly, 48 hours after siRNA transfection, 2×10^5 pericytes with 1.0×10^6 PMVECs were suspended in chilled 500 μL/plug of Matrigel growth factor−reduced solution (BD Biosciences), to which 50 μg/mL fibroblast growth factor (FGF) (100-18B; PeproTech Inc., Rocky Hill, NJ) was added. Plugs were implanted in the backs of severe combined immunodeficiency (SCID) mice (Charles River Laboratories International, Inc., Wilmington, MA) anesthetized by s.c. injection of ketamine/xylazine. For each experimental condition, a total of two plugs were implanted in each animal and allowed to remain in place for 14 days. At the end of this period, the animals were humanely sacrificed, and the Matrigel plugs were removed and fixed in 4% paraformaldehyde for 24 hours before paraffin embedding. Unstained tissue samples were double-labeled with Alexa Fluor 488−labeled anti-human CD31 (LS-B4737, LifeSpan Biosciences, Inc., Seattle, WA) and Alexa Fluor 555−labeled anti-mouse CD31 (catalog number 553370, BD Biosciences) to identify human or murine ECs, Cy3-α-SMA (C6198; Sigma-Aldrich) to identify pericytes, and DAPI for nuclear staining. Ten images per slide were captured using the 40× objective of DMRB II fluorescence inverted microscope and analyzed using LAS X software version 1.1.0 (Leica Microsystems Inc.). The presence of microvessels (defined as tubes filled with red blood cells) was documented using hematoxylin and eosin section, and the numbers of human and murine cells and pericytes per condition were quantified using the aforementioned immunofluorescence techniques.

Live-Imaging Video Microscopy

Cells were allowed to attach and spread on glass coverslips in the incubator and were viewed on an inverted microscope (DMRB II; Leica Microsystems, Inc.). The microscope is also equipped with a heated stage, differential interference contrast optics, and epifluorescence. Filters and light paths were controlled with a filter wheel and shutters (Ludl Electronic Products Ltd., Hawthorne, NY). For green and red fluorescent protein visualization, a single-band excitation filter for fluorescein isothiocyanate and Texas Red, respectively, were used. Tissue culture medium without phenol red was kept warm and buffered in a CO_2 incubator. The stage temperature was kept at 37°C with an automatic thermostat. Images were collected using a charge-coupled device camera (C2400; black and white) with on-chip integration and a digital image processor (Argus 20; PerkinElmer, Waltham, MA). Acquired images were assembled in temporal sequences using Leica software and saved as QuickTime videos (Apple, Inc., Cupertino, CA). The path traveled by the cells was calculated by recording the position of the nucleus in individual frames using ImageJ software version 1.44p (NIH, Bethesda, MD) and plotting on an *xy* axis followed by measurement of the distance between each of the individual points.

Statistical Analysis

Values from multiple experiments are expressed as means ± SEM. Statistical significance was determined using either an unpaired *t*-test or one-way analysis of variance followed by Bonferroni multiple comparison tests unless stated otherwise. $P < 0.05$ was considered significant.

Results

Isolation and Characterization of Pericytes from Healthy Donor and PAH Lungs Using Recombinant 3G5 IgG−Coated Magnetic Beads

Previous studies have reported successful isolation of pericytes from tissues such as skin[13] and lungs[11] using anti−3G5 IgM coupled magnetic beads. In our hands, this

method led to inconsistent pericyte yields per isolation, likely due to IgM polymerization during storage. In an effort to develop a more reliable and reproducible isolation method, we sequenced the variable domains of the 3G5 IgM and cloned them into a murine IgG backbone followed by magnetic bead coupling (Figure 1A). Compared to 3G5 IgM, the yield of pericytes obtained using the 3G5 IgG was significantly greater (>20%) and more consistent per isolation. In culture, pulmonary pericytes extend numerous cell processes when seeded in Matrigel while displaying a smooth muscle cell (SMC)-like morphology when attached to gelatin-coated plates (Figure 1A). To validate pericyte lineage, we used fluorescence-activated cell-sorting analysis to document the expression of well-known pericyte markers such as NG2, 3G5, CD90/thymus cell antigen 1, CD146, PDGFRβ, calponin, α-SMA, and SM22α, as well as the absence of other lineage markers such as CD31 and CD45, which are

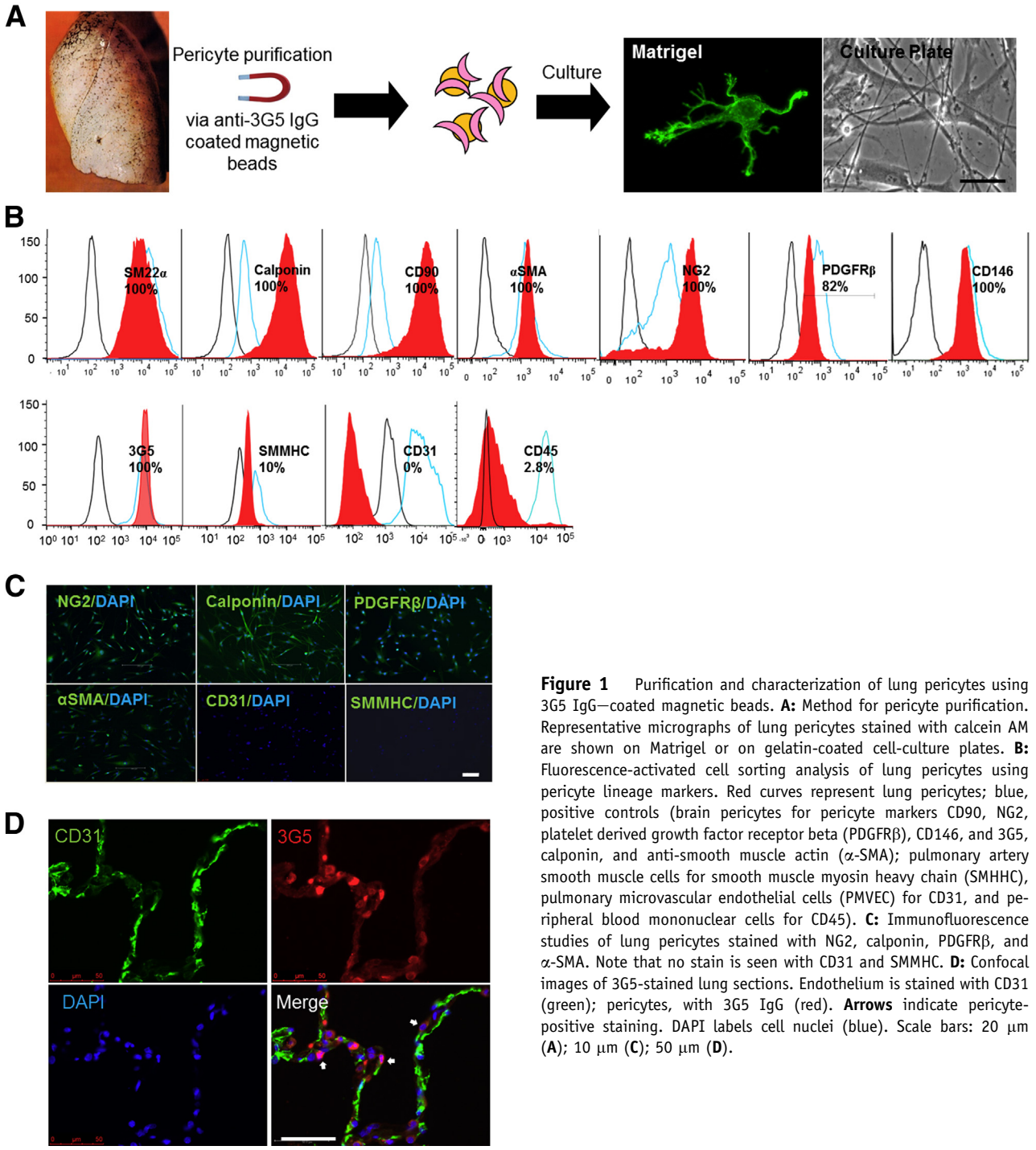

Figure 1 Purification and characterization of lung pericytes using 3G5 IgG—coated magnetic beads. **A:** Method for pericyte purification. Representative micrographs of lung pericytes stained with calcein AM are shown on Matrigel or on gelatin-coated cell-culture plates. **B:** Fluorescence-activated cell sorting analysis of lung pericytes using pericyte lineage markers. Red curves represent lung pericytes; blue, positive controls (brain pericytes for pericyte markers CD90, NG2, platelet derived growth factor receptor beta (PDGFRβ), CD146, and 3G5, calponin, and anti-smooth muscle actin (α-SMA); pulmonary artery smooth muscle cells for smooth muscle myosin heavy chain (SMHHC), pulmonary microvascular endothelial cells (PMVEC) for CD31, and peripheral blood mononuclear cells for CD45). **C:** Immunofluorescence studies of lung pericytes stained with NG2, calponin, PDGFRβ, and α-SMA. Note that no stain is seen with CD31 and SMMHC. **D:** Confocal images of 3G5-stained lung sections. Endothelium is stained with CD31 (green); pericytes, with 3G5 IgG (red). **Arrows** indicate pericyte-positive staining. DAPI labels cell nuclei (blue). Scale bars: 20 μm (**A**); 10 μm (**C**); 50 μm (**D**).

present mainly in ECs and leukocytes, respectively (Figure 1B). It is also worth noting that pericytes could be distinguished from SMC by their lack of expression of smooth muscle myosin heavy chain,[14] a lineage marker expressed mainly by differentiated SMC (Figure 1B). Finally, the expression of the pericyte markers NG2, calponin, PDGFRβ, and α-SMA was further confirmed by immunofluorescence in cultured lung pericytes (Figure 1C). Finally, in agreement with previous reports,[11] we found that 3G5 IgG labels mural cells adjacent to lung capillaries (Figure 1D) in a manner comparable to that of its IgM counterpart (data not shown).

Establishment of Endothelial−Pericyte Interactions by PAH Pericytes Is Significantly Reduced in a Matrigel Co-Culture Model

Pericytes are known to provide mural support and promote vessel stabilization. Whether PAH pericytes display an abnormal phenotype in this regard is unknown. To test this, we co-cultured healthy PMVECs with either healthy donor or PAH pericytes at a 5:1 ratio in Matrigel, a biological matrix that promotes tube formation by ECs *in vitro*.[15] Compared to PMVECs alone (Figure 2A), co-culture with healthy pericytes resulted in a threefold increase in the size of the tube networks, as evidenced by the total numbers of tubes, branching points, and loops ($P < 0.05$) (Figure 2B). In contrast, co-culture of healthy PMVECs with PAH pericytes under the same conditions resulted in a vascular network that was no different in size as that seen when PMVECs were cultured alone (Figure 2C). To determine whether the observed difference in network size was associated with a difference in pericyte distribution, we stained pericytes with a red (PKH26) and PMVECs with a green (PKH67) cell membrane dye (see *Materials and Methods*) and visualized them in co-culture. We found that healthy pericytes established contacts with ECs mostly along the length of the vascular tubes (Figure 2B), whereas PAH pericytes tended to cluster away from the vascular tubes either within the nodes or outside in the Matrigel (Figure 2C).

Based on our findings, we speculated whether a motility defect could account for the abnormal PAH pericyte distribution seen in the Matrigel co-culture. To test this, we used live-imaging video microscopy (LVM) to monitor the behavior of PKH26-labeled pericytes and PKH67-labeled PMVECs during the assembly of the vascular tube network. As expected, healthy donor pericytes demonstrated vigorous polarization and migration toward the developing endothelial tubes that would culminate in pericyte association to the outer layer of the tubes (Supplemental Figure S1A and Supplemental Movie S1). In contrast, most PAH pericytes failed to demonstrate either polarization and/or spontaneous motility toward adjacent areas where endothelial tubes were being formed (Supplemental Figure S1B and Supplemental Movie S2).

PAH Pericytes Demonstrate Reduced Motility and Slow Cytoskeletal Rearrangements

Cell motility is a complex behavior characterized by dynamic changes in cell shape made possible by active rearrangement of the cytoskeleton.[16] To further delineate the cell shape patterns of healthy donor and PAH pericytes during spontaneous cell movement, we used LVM to monitor pericyte monocultures over 4 hours and tracked both the movement and cell shape changes occurring in both healthy donor and PAH during that time period. Compared to their healthy counterparts, PAH pericytes were significantly slower and traced shorter cell paths (Supplemental Figure S1C). A closer look at cell morphology during this time period revealed that healthy pericytes display active exploratory behavior as demonstrated by the presence of wide and dynamic lamellipodia at their front end and propulsive activity associated with contraction along the longitudinal cell axis (Supplemental Figure S1D and Supplemental Movie S3). In contrast, PAH pericytes demonstrated much narrower and less dynamic filopodia and lamellipodia that connected to the main cell body via a long cytoplasmic process, resulting in a much longer and narrower body axis (Supplemental Figure S1D and Supplemental Movie S4). Furthermore, these cells also appeared to be less contractile and remained attached to a given area longer, which could account for their limited ability to cover the same distance as healthy donor cells.

PAH Pericytes Display Reduced Polarization toward PMVEC Monolayers

To properly carry out its assigned role in angiogenesis, a pericyte must be capable of migrating toward emerging blood vessels. This event is triggered by secreted factors (eg, PDGF, FGF) released by ECs, which help polarize the pericyte toward the blood vessel.[1,17] A key finding in our LVM co-culture studies was the apparent lack of polarization of PAH pericytes toward the endothelial tubes, leading us to investigate whether polarization was abnormal in these cells. Using a modified Boyden chamber assay, we seeded either healthy donor or PAH pericytes on top of the 8-μm porous membrane followed by placement inside a 24-well plate containing healthy PMVECs (Figure 2E). In the absence of PMVECs, healthy donor pericytes spontaneously transmigrated in significantly greater numbers compared to PAH cells, a phenomenon that was significantly enhanced when the pericytes were co-cultured with PMVECs (Figure 2E).

Although the Boyden chamber assay is designed to test chemotaxis in response to a stimulus (eg, PMVEC derived growth factors), it does not provide information concerning cytoskeletal rearrangements required to ensure polarization toward the source of the stimulus. To complement our Boyden chamber studies, we also performed wound-healing studies designed to assist us in measuring pericyte polarity

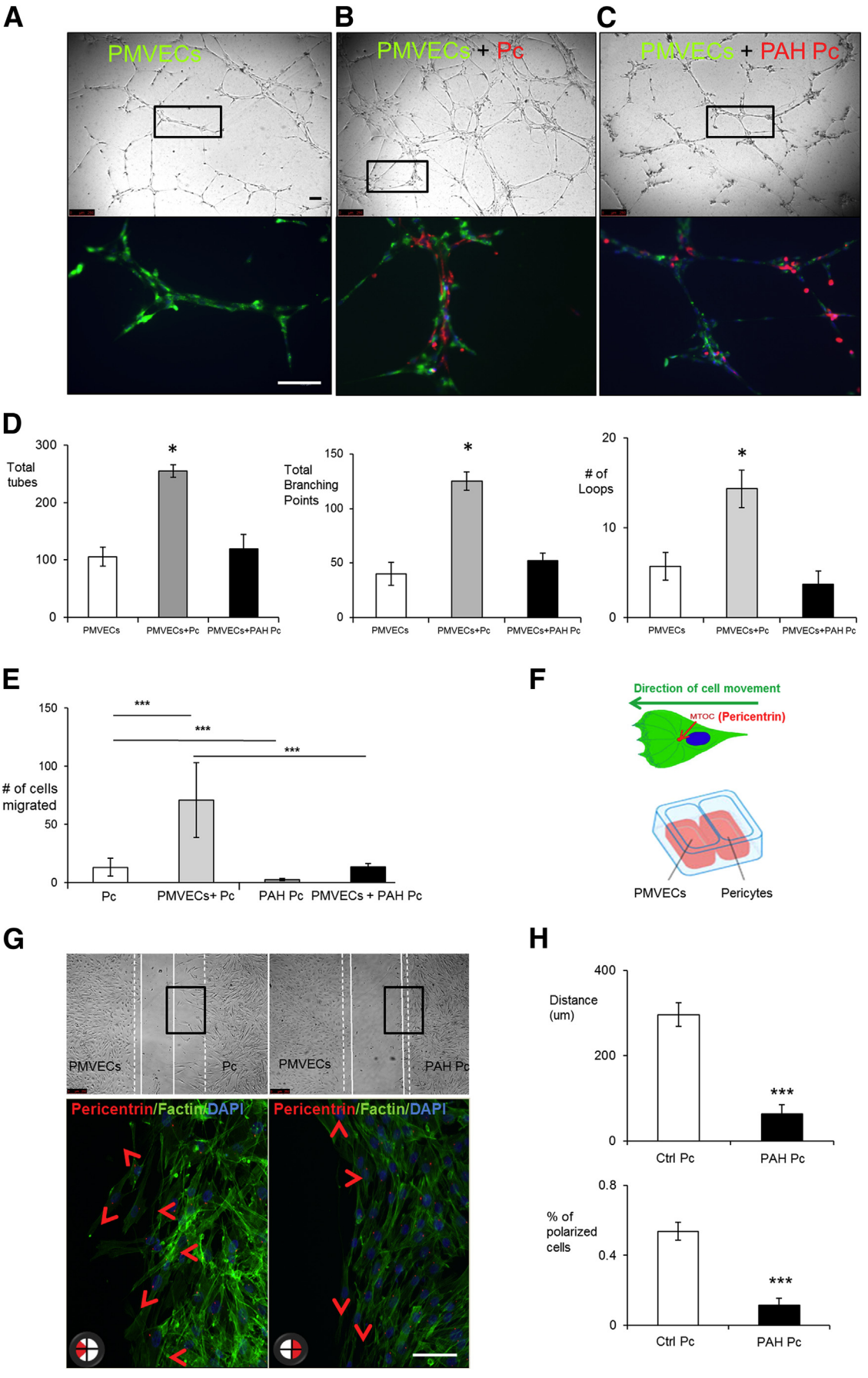
A
B
C
PMVECs
PMVECs + Pc
PMVECs + PAH Pc
D
Total tubes
Total Branching Points
# of Loops
PMVECs
PMVECs+Pc
PMVECs+PAH Pc
E
# of cells migrated
Pc
PMVECs+ Pc
PAH Pc
PMVECs + PAH Pc
F
Direction of cell movement
MTOC (Pericentrin)
PMVECs
Pericytes
G
PMVECs
Pc
PAH Pc
Pericentrin/Factin/DAPI
H
Distance (um)
Ctrl Pc
PAH Pc
% of polarized cells

in response to PMVECs. Using a wound-healing assay optimized to allow co-culture of PMVECs and pericytes (Figure 2F), we measured the degree of cell polarization by staining pericytes for pericentrin, a protein located within the MTOC. During cell motility, the MTOC is localized to the front of the nucleus and aligns itself with the long axis of the cells, thus helping to identify the direction of cell movement.[18] After 6 hours, we saw that the MTOC of most healthy pericytes close to the wound edge pointed toward the PMVECs in the opposite side, and that the pericytes initiated movement in that direction, as evidenced by narrowing of the wound gap during this time (Figure 2G). In contrast, PAH pericytes demonstrated a threefold more random MTOC orientation along the length of the wound edge, which correlated with a fourfold decrease in wound gap narrowing after 6 hours of culture (Figure 2, G and H).

The Wnt/PCP Pathway Is a Candidate Pathway that Regulates Pericyte Motility and Polarity during Angiogenesis

As our next step, we sought to investigate the mechanisms that regulate pericyte motility and polarization, with the goal of identifying possible genetic abnormalities that contribute to the observed abnormal phenotype of PAH pericytes. Using co-culture studies similar to ours, investigators have identified key roles for multiple signaling pathways in promoting pericyte recruitment to ECs during angiogenesis. At present, it is thought that growth factors released by ECs trigger signaling pathways within pericytes that ultimately result in their association to blood vessels.[3,19] Among these, FGF and PDGF are the best established signaling pathways for this role as mutations that alter pathway activation at any level and result in reduced pericyte recruitment to blood vessels. To test whether the motility response of healthy donor and PAH pericytes occurs in response to these ligands, we used a conventional Boyden chamber assay to measure pericyte transmigration in response to 20 ng/mL PDGF or 10 ng/mL FGF over 6 hours. While pericyte transmigration was more robust in the healthy donor cells, PAH pericytes also demonstrated a chemotactic response to both ligands (Figure 3, A and B). This finding led us to speculate whether other candidate pathways could have a more pronounced role in the recruitment of pericytes to pulmonary vessels.

Among possible candidate pathways, we prioritized the Wnt/PCP pathway for a number of reasons. Originally described in *Drosophila*, the Wnt/PCP pathway is involved in coordinating directional cell movements during development and orchestrating cell polarity across epithelial surfaces.[20] Wnt ligands interact with Fzd receptors in the cell surface to trigger downstream activation of the small GTPases RhoA, Rac1, and cdc42, which then coordinate the cytoskeletal rearrangements necessary to affect cell movement and polarization. Based on this information, we asked whether Wnt/PCP signaling could be involved in steering pericytes toward nascent pulmonary arteries.

As a first step, we used the Boyden chamber approach to measure the chemotactic response of healthy donor and PAH pericytes to recombinant Wnt5a, a ligand known to activate the Wnt/PCP pathway[20] and known to be expressed in ECs, where it helps to coordinate tight junction integrity and cell polarity.[21] Surprisingly, we found that 100 ng/mL recombinant Wnt5a induced significant translocation of healthy pericytes across the Boyden membrane over a period of 6 hours. In contrast, PAH pericytes failed to demonstrate any significant motogenic response to Wnt5a (Figure 3, A and B). To measure Wnt/PCP activation in response to Wnt5a, we stimulated healthy donor and PAH pericytes with Wnt5a over 4 hours and measured levels of active RhoA, Rac1, and cdc42 in cell lysates. As anticipated, we found a significant increase in activity in all three GTPases in Wnt5a-stimulated healthy donor cells, whereas no significant activation was found in PAH pericytes (Figure 3, C and D).

Expression of Wnt/PCP Components Fzd7 and cdc42 Is Reduced in PAH Pericytes

We sought to characterize the expression profile of all known Wnt/PCP genes[22] in both healthy donor and PAH pericytes using TaqMan quantitative PCR and to determine whether gene-expression patterns differed between the two groups. Using this approach, we found the Wnt/PCP genes that were either up-regulated or down-regulated (Figure 3E) in PAH pericytes compared to healthy donor pericytes. The most striking difference was found in the expression of Fzd7, a

Figure 2 Pulmonary arterial hypertension (PAH) pericytes (Pc) fail to associate with pulmonary microvascular endothelial cells (PMVECs) during vascular tube formation and demonstrate reduced polarization to the endothelial monolayer in both Boyden chamber and wound-healing co-culture assays. Matrigel assays show tube formation by PMVEC (PKH67, green) alone (**A**) and in the presence of pericytes (Pc) (PKH26, red) from healthy donors (**B**) or from PAH patients (**C**). **Bottom row** shows enlargements of the **boxes** in the **top row**. Note that pericyte distribution is seen along the length of vascular tubes with healthy pericytes, whereas it appears clustered around nodes with PAH pericytes. **D:** Numbers of tubes (**left**), branching points (**middle**), and loops (**right**) with PMVECs without and with pericytes from healthy subjects (control) or from PAH patients. **E:** Boyden chamber comparing translocation of control Pc and PAH pericytes (PAH Pc) in the presence or absence of PMVECs. After 6 hours, pericytes at the bottom of the inserts were fixed and stained with hematoxylin and eosin. The mean number of pericytes from four random 20× fields was used for comparison. **F:** Estimation of polarization using pericentrin, a marker of the microtubule organization center, and of the wound-healing co-culture assay. **G:** Representative images of wound-healing co-culture assays in which PMVECs are on the left and pericytes on the right. **Bottom row** shows enlargements of the **boxes** in the **top row**. Cell polarity was assessed by pericentrin (red section in circle at the bottom left of each panel indicates direction). The **dashed lines** indicate 0 hours; **white lines**, 6 hours. The **arrowheads** indicate directions of cell movement. **H:** Quantification of cell distance and percentage of polarized cells after 6 hours. Data are expressed as means ± SEM of three experiments. $^{*}P < 0.05$ versus PMVEC alone (one-way analysis of variance with Dunnett post-test); $^{***}P < 0.001$ [one-way analysis of variance with Bonferroni post-test (**E**)] or versus control [Ctrl; unpaired *t*-test (**H**)]. Scale bars = 100 μm.

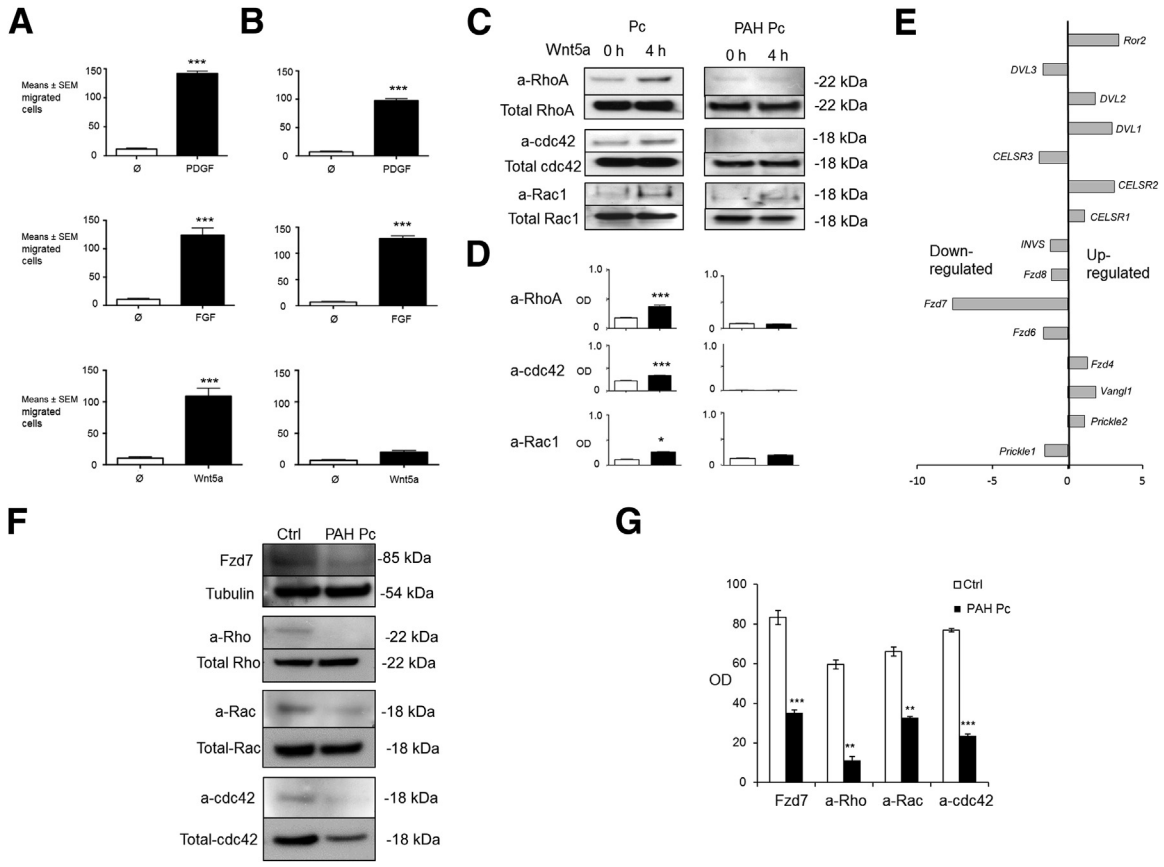

Figure 3 Reduced Wnt/planar cell polarity activation is present in PAH pericytes. Boyden chamber assays of pericytes from healthy donors (**A**) and PAH patients (**B**), stimulated (black bars) with 20 ng/mL PDGF (**top row**), 10 ng/mL FGF (**middle row**), and 200 ng/mL Wnt5a (**bottom row**) over 6 hours. White bars represent nonstimulated cells (control). **C:** Pull-down assays measuring active (a) forms of RhoA, cdc42, and Rac1 in lysates of Wnt5a-stimulated pericytes from healthy donors (Pc) and PAH patients (PAH Pc) over a period of 4 hours. **D:** Densitometry values are shown as the ratios of the optical density of the active form relative to the respective total GTPase in whole cell lysates that were run in C gels. The white bars represent no Wnt5a stimulation; black bars, 4-hour Wnt5a stimulation. **E:** TaqMan quantitative PCR for Wnt/PCP-related components in PAH pericytes. The expression of each gene is shown relative to that in healthy pericytes. **F:** Representative Western immunoblot images of Fzd7 and cdc42 in whole lysates of pericytes from healthy donors (Ctrl) versus PAH patients (PAH Pc). **G:** Densitometry values are shown as the ratio of the optical density of the active form relative to the respective total GTPase in whole cell lysates. Blots were probed for total GTPase as a loading control. Data are expressed as means ± SEM of three experiments. $*P < 0.05$, $**P < 0.01$, and $***P < 0.001$ versus control [unpaired *t*-test (**D**), one-way analysis of variance with Bonferroni post-test (**G**)].

member of the Fzd family of seven-pass transmembrane receptors that binds Wnt ligands at the surface and activates downstream mediators of the various Wnt pathways.[23] Several studies have shown that Fzd7 is capable of activating the Wnt/PCP pathway to coordinate myogenic stem cell motility[24] as well as heart[25] and body axis formation[26] in early mammalian development, and that its deficiency can result in congenital disorders such as ventricular septal defect.[25] Western blot analysis of lysates from PAH pericytes obtained after co-culture with PMVECs revealed a significant reduction in Fzd7 that correlated with low levels of active RhoA, Rac1, and cdc42 activity as seen by pull-down assays (Figure 3, F and G). Whereas levels of total RhoA and Rac1 were comparable between healthy and PAH pericytes, cdc42 expression was significantly reduced in PAH.

To test whether Fzd7 deficiency could account for loss of Wnt/PCP activation in PAH pericytes, we used siRNA to knockdown Fzd7 expression in healthy pericytes to levels comparable to those in PAH cells. Surprisingly, when co-cultured in Matrigel with healthy PMVECs, we found that Fzd7-deficient pericytes were still capable of associating with endothelial tubes in a manner comparable to that of control siRNA-treated pericytes (Figure 4A), leading us to question whether loss of Fzd7 alone is not sufficient to explain the PAH pericyte phenotype.

Knockdown of Both Fzd7 and cdc42 Suppresses Pericyte Motility and Polarization

One of the most dramatic findings in our characterization of PAH pericytes was their inability to properly polarize toward the endothelium, as documented via LVM and wound-healing assays. Among the downstream mediators of Wnt/PCP activity, cdc42 is known to be essential for cell polarity as it can help coordinate the proper location of actin filaments to steer the cell in the right direction, and mutations that reduce either level or activity of this small GTPase can result in severe defects in cell polarization and motility.[27,28] Furthermore, of the

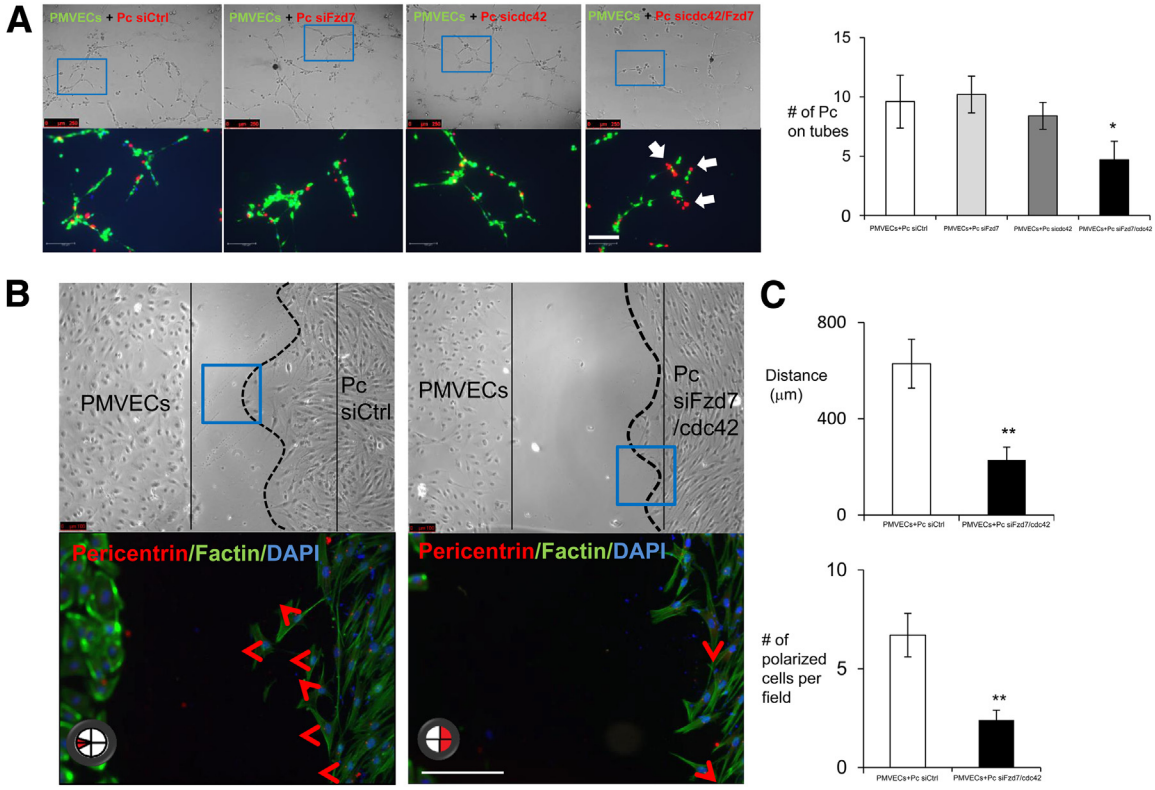

Figure 4 Knockdown of both Fzd7 and CDC42 in healthy pericytes shows impaired tube formation and cell polarity. **A:** Pericytes (Pc) were transfected with nontargeting siRNA control (siCtrl), siFzd7, sicdc42, and siFzd7/cdc42 for 48 hours. Before seeded on Matrigel, cells were stained with PKHs. PMVEC were stained in PKH67, green; Pc in PKH26, red; and DAPI in blue. The **blue boxes** indicate the enlarged areas of magnification in the bottom row. The **white arrows** indicate the interaction of EC-Pc. Tube formations and the numbers of pericytes attached to the tubes were assessed after 6 hours. **B:** Polarity was also assessed and measured on single or double knockout in healthy pericytes. The **red arrowheads** indicate directions of cell movement. **C:** Cell movement distances and percentages of polarized cells were quantified when siFzd7/cdc42 were transfected on control pericytes. Data are expressed as means ± SEM of three experiments. $*P < 0.05$, $**P < 0.01$ versus control (unpaired *t*-test). Scale bars = 100 μm.

three small GTPases targeted by Wnt/PCP, only cdc42 demonstrated reductions in both activity and total protein levels in PAH cells (Figure 3, F and G). To test whether cdc42 deficiency could impair pericyte recruitment to endothelial tubes, we used siRNA to knock down cdc42 in healthy pericytes and performed co-culture studies with healthy PMVECs. Similar to the Fzd7 siRNA–treated cells, the cdc42 siRNA–treated pericytes failed to recapitulate the phenotype of PAH pericytes, as they also were capable of associating with the endothelial tubes (Figure 4A).

One possible explanation for the lack of effect seen in either Fzd7 or cdc42 siRNA–treated pericytes is the possibility of compensation by other Fzd receptors present in the pericyte membrane as well as parallel activation of other signaling pathways (eg, PDGF[29] and FGF[30]) involved in pericyte recruitment to ECs that also target cdc42, thus compensating for reduced Wnt/PCP signaling. To test this, we generated Fzd7/cdc42 siRNA double-knockdown pericytes (Supplemental Figure S2, A and B) and measured their ability to associate with endothelial tubes in co-culture. In contrast to either Fzd7 or cdc42 siRNA–treated cells, the ability of Fzd7- or cdc42-deficient pericytes to properly migrate and attach to endothelial tubes was reduced by twofold, a finding that closely recapitulated the behavior of PAH pericytes (Figure 4A). We further tested the effect of Fzd7/cdc42 knockdown on pericyte polarization in response to PMVECs using our modified wound-healing co-culture assay and demonstrated that, similar to PAH pericytes, proper polarization of Fzd7- or cdc42-deficient cells was decreased by 2.5-fold and that movement to the endothelium was reduced by 2.8-fold (Figure 4, B and C).

Reduced Fzd7 and cdc42 Expression Prevents Pericyte Association to Blood Vessels in SCID Mice

Our current studies indicate that dual Fzd7 and cdc42 depletion can impair pericyte motility and polarity toward PMVECs and that PAH cells have decreased Fzd7 and cdc42. However, whether this is relevant to *in vivo* establishment of endothelial–pericyte interactions and their failure in PAH is unknown. To study endothelial–pericyte behavior *in vivo*, we suspended co-cultures of PMVECs with healthy pericytes transfected with either nontargeting or Fzd7/cdc42 siRNA in Matrigel plugs and implanted them on the backs of SCID mice for 14 days before extraction, a well-established model for the study of *in vivo* angiogenesis[31] (see *Materials and Methods*). Compared to PMVECs-only plugs (Figure 5A), co-cultures of PMVECs

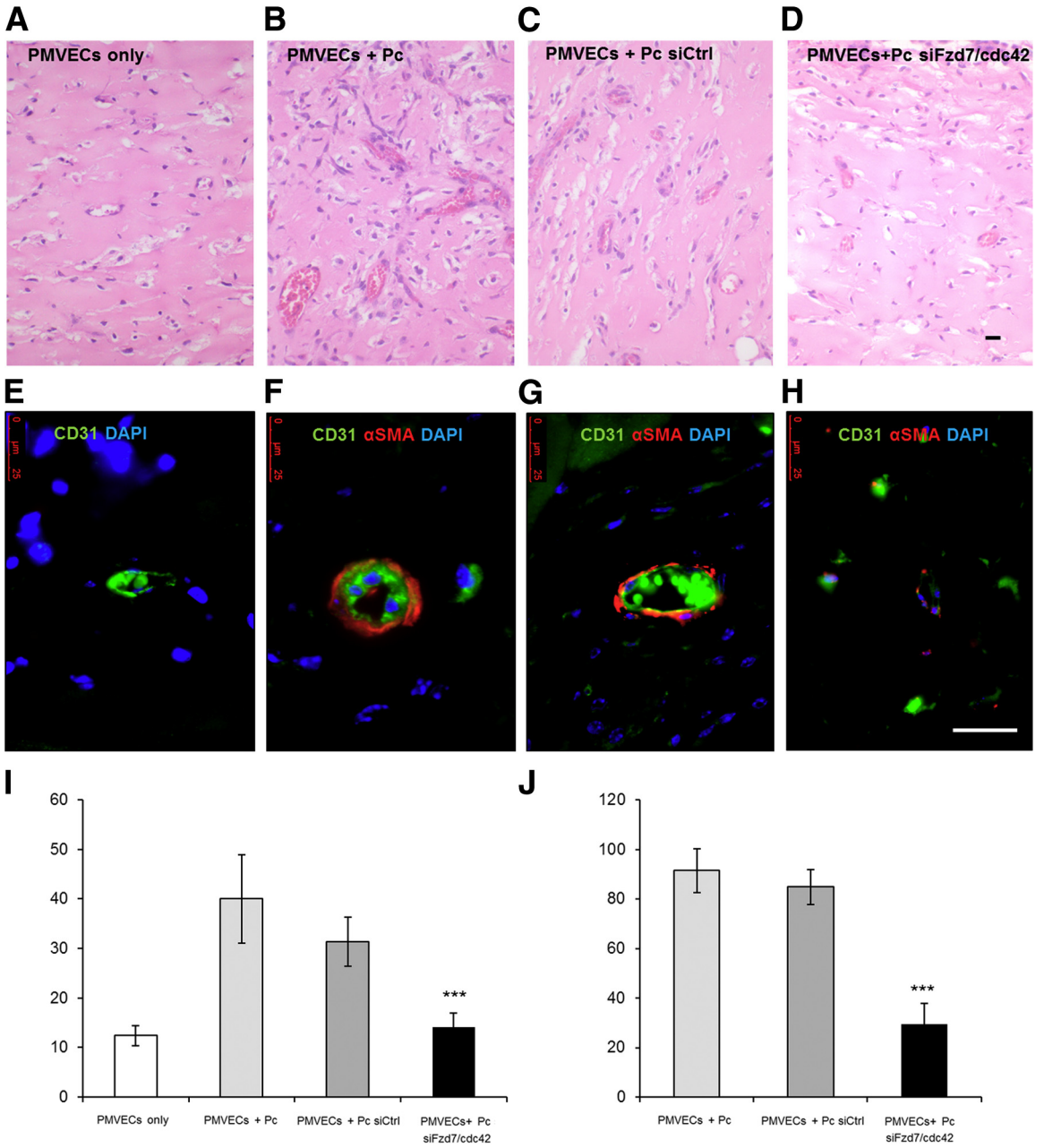

Figure 5 Reduction of Fzd7 and cdc42 prevents pericyte-induced microvessel formation in SCID mice. Representative images of hematoxylin and eosin staining (**A**–**D**) and immunofluorescence (**E**–**H**) show the appearance of PMVECs alone (**A**), PMVECs plus healthy pericytes (Pc) (**B**) as positive controls, PMVECs plus healthy pericytes transfected with siRNA control (siCtrl) (**C**), and PMVECs plus healthy pericytes transfected simultaneously with siFzd7 and sicdc42 (**D**) 14 days after implantation into SCID mice. **E**–**H:** Human and murine CD31 is labeled with green fluorescent antibodies, pericytes are labeled with α-SMA-Cy3 red fluorescent antibodies, and nuclei are stained blue with DAPI. Quantification of vessel diameter (**I**) in micrometers and the percentage of pericyte coverage (**J**). Data are expressed as means ± SEM of three experiments. ***$P < 0.001$ versus PMVECs + Pc siCtrl. Scale bar = 25 μm.

with pericytes transfected with nontargeting siRNA resulted in blood-filled vessels with larger diameters (Figure 5C) and complete mural coverage by pericytes, as evidenced by positive α-SMA staining around the CD31-positive ECs (Figure 5G). In contrast, plugs containing PMVECs and Fzd7/cdc42 siRNA–treated pericytes (Figure 5D) contained twofold smaller blood-filled vessels that were similar in appearance to those in the PMVEC-only plugs (Figure 5, A and I) and less than 2.6-fold pericyte coverage as evidenced by minimal circumferential α-SMA staining (Figure 5, H and J).

Restoration of Fzd7 and cdc42 Improves Establishment of Endothelial-Pericyte Interactions by PAH Pericytes in a Matrigel Co-Culture Model

To determine whether restoring Fzd7 and cdc42 expression in PAH pericytes could increase Wnt/PCP activity and

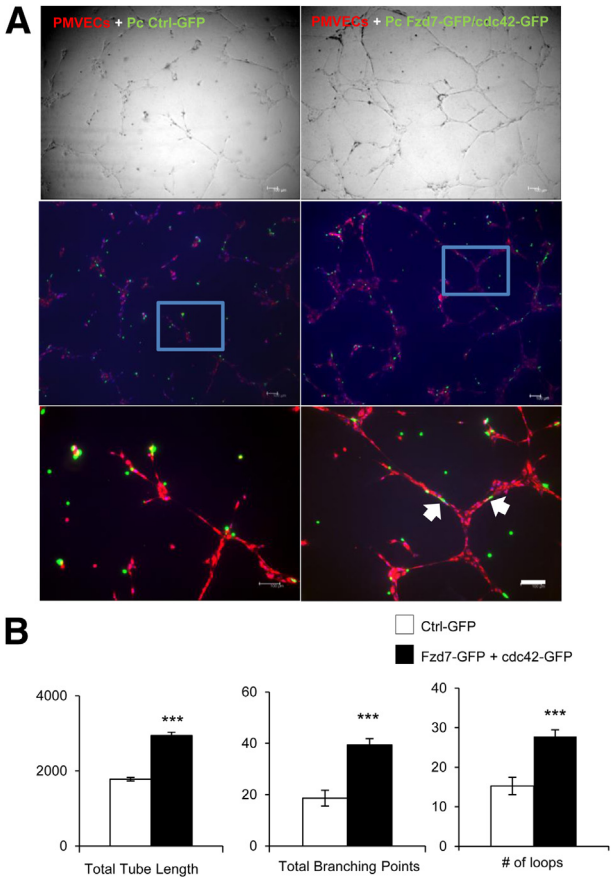

Figure 6 Transfection of Fzd7 and cdc42 expression constructs in PAH pericytes improve their ability to associate with vascular tubes. **A:** PAH pericytes were transfected with GFP-tagged Fzd7 and cdc42 plasmids (green) and seeded with PMVECs (red) in Matrigel-coated plates (**top row**). **Bottom row** shows enlargements of the **boxes** in the **middle row**. The **white arrows** indicate the interaction of EC-Pc. **B:** Quantification of total tube lengths in micrometers (**left**), total number of branching points (**middle**), and numbers of loops (**right**). Data are expressed as means ± SEM of three experiments. $***P < 0.001$ versus control (Ctrl-GFP). Scale bar = 100 μm.

improve their ability to associate with endothelial tubes, we transfected plasmids containing wild-type Fzd7-GFP and cdc42-GFP into PAH pericytes followed by co-culture with healthy PMVECs in Matrigel. As anticipated, compared to cells transfected with empty vector, Matrigel co-cultures of PMVECs with wild-type Fzd7 + cdc42–transfected PAH pericytes demonstrated an increase in tube network size, as evidenced by a significant increase in the total length of tubes, total branching points, and number of loops (Figure 6, A and B). As anticipated, PAH pericytes were now able to wrap around endothelial tubes and enhance PMVECs to form wider tubes, as seen in co-culture studies with healthy pericytes (Figure 2B).

Discussion

Until recently, most of our understanding of lung pericyte distribution came from the study by Weibel,[32] which reported sparse distribution of these cells mainly along the perialveolar capillaries and venules. In 2014, investigators reported that pericyte numbers appeared to be increased in the pulmonary microcirculation of PAH patients and that this pattern appeared to correlate with muscularization of distal vessels.[11] The link between pericytes and small vessel muscularization in PAH has been proposed by investigators looking at lung sections of PAH patients with congenital heart conditions[33] as well as in transgenic murine models of SM22α-mediated *BMPR1A* deletion.[34] Our present study provides new insight into the biology of these enigmatic cells and their possible contribution to the progressive loss of small pulmonary arteries seen in PAH. We also introduce a key role for the Wnt/PCP signaling pathway in helping pericytes to associate with developing blood vessels and identify two key genes within this pathway whose reduced expression severely impairs the ability of PAH pericytes to provide mural coverage (Figure 7).

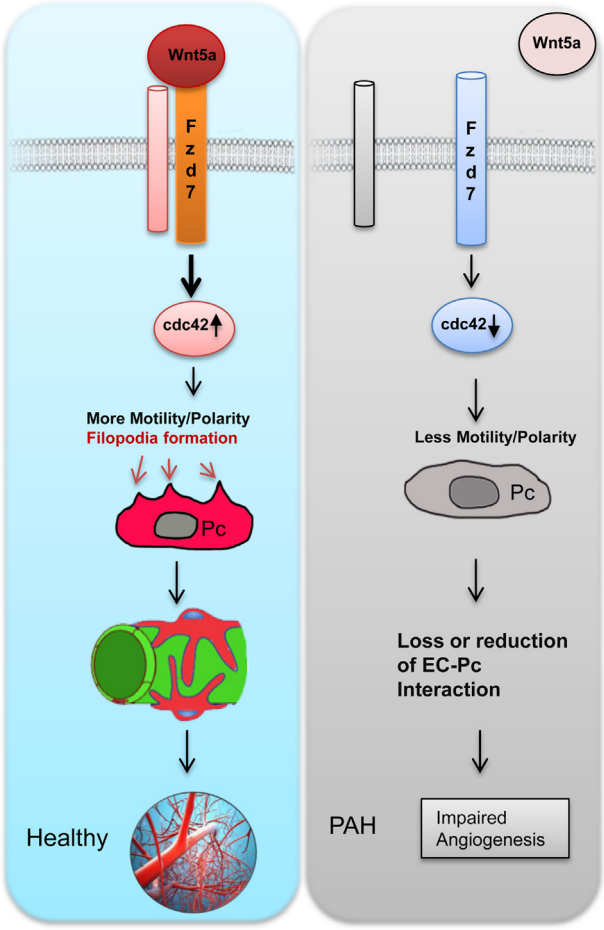

Figure 7 Model representing that Wnt/planar cell polarity signaling contributes to the association between pericytes and developing blood vessels via the Wnt5a-Fzd7-cdc42 axis. The up-regulation of cdc42 on Wnt5a/Fzd7 signaling results in increased motility and polarity, which in turn results in healthy growth. A lack of Wnt5a/Fzd7 signaling results in less motility and polarity, which in turn leads to a loss or reduction of the interaction between endothelial cells (EC) and pericytes (Pc) and eventually a loss of arteries, leading to PAH.

The major shortcoming of pericyte-isolation techniques is the presence of contaminating cell populations and the inability to distinguish pericyte phenotype from other contaminating cells. Our approach to isolate pericytes from lung tissue using modified anti−3G5 IgG antibodies conjugated to magnetic beads was modified from a previously published protocol.[13] We found that this chimeric antibody: i) has a longer (>3 months) shelf life, ii) has reliable performance, and iii) is compatible with a wide range of applications. To confirm the pericyte lineage of the lung cells isolated using the chimeric 3G5 IgG, we used fluorescence-activated cell sorting to document the expression of a wide range of lineage markers known to be expressed by pericytes. In our study, 10 fluorophore conjugated antibodies were stained simultaneously on a single cell. However, we must recognize that this is still a narrow selection of markers and that there are more pericyte markers that need to be further evaluated, such as inter-cellular adhesion molecule, Nestin, regulator of G-protein signaling 5, vascular cell adhesion molecule 1, Vimentin, which will be the subject of our future studies.[17] Our study is also limited in that we did not look for dedifferentiated cells in our population, an issue that could be relevant especially when we consider that pericytes have been suggested by some investigators to behave as pluripotent and mesenchymal-like cells in some settings.[3] Future studies should look carefully at the effects of culture condition, cell density, and signaling factors that could influence the potential of the pericytes to change into other cell types under various cell-culture conditions.

One of the most striking findings in this study is the limited association of PAH pericytes with vascular tubes seen in the Matrigel co-culture assays. Use of co-culture methods has remained a viable and useful strategy to study endothelial-pericyte interactions *in vitro* as it provides not only the opportunity to study signaling pathways but also to visually capture the behavior of both cell types in real time.[19,35−37] Furthermore, vascular networks assembled in co-culture models have greater longevity compared to those made by ECs alone.[19,36] Although the use of the Matrigel matrix for the study of angiogenesis is well documented, it is important to point out that its protein composition and growth factor content[15] may be significantly different from what is found in the lung and could influence the cell behavior in co-culture. However, it is pertinent to mention that we were able to reproduce the behavior of PAH pericytes when cultured in collagen,[36] hydrogel,[38] and fibrin[39] based matrices (data not shown), leading us to conclude that the phenotype observed in our Matrigel studies is an inherent feature of these cells. These findings are relevant in light of the recent report stating an increase in pericyte numbers in the pulmonary microcirculation of PAH patients.[11] Although this study supports the presence of pericyte-like cells around the vessels, it is unclear to what extent these cells are in direct physical contact with the ECs within these vessels. This is clinically relevant as a lack of physical contact could reduce vessel viability and result in small vessel loss, a pertinent pathological feature of PAH.[40,41]

The use of LVM and wound-healing assays provided important information concerning the behavior of pericytes during the assembly of vascular networks and led us to identify a defect in both motility and polarity in PAH pericytes. Cell motility is a highly dynamic cellular event that requires the relocation and assembly of cytoskeletal components and is tightly controlled by the temporal activation of small GTPases such as RhoA, Rac1, and cdc42.[27] We found that, in contrast to healthy cells, PAH pericytes appeared to move slower and demonstrate persistence in their attachment to a given region of the culture plate (Supplemental Figure S1). In addition, it was also evident that most of the PAH pericytes could not generate wide lamellipodia, a structure that assists cell motility by helping to provide forward traction to the front end of the cell and whose absence is known to compromise the speed, distance, and persistence of cell movement.[42] This observation is in contrast with reports of increased PAH pericyte motility when exposed to endothelial conditioned media.[11] However, it is worth pointing out that we always used healthy PMVECs in all of the co-culture assays and the production of mediators from these cells is open to the influence of mediators produced by pericytes, a situation that was developed to recapitulate the way these two cell types are thought to interact during angiogenesis. This is particularly relevant when we consider that co-culture studies of healthy pericytes with PAH PMVECs also demonstrated an impairment of pericyte association with vascular tubes (data not shown), thus supporting a crucial role for the ECs in driving recruitment of pericytes.

Signaling cascades between pericytes and ECs have been studied extensively using genetic mouse models. To point out a few: i) PDGFβ/PDGFRβ signaling mediates pericyte recruitment,[43] ii) transforming growth factor β signaling has been implicated in both mural and EC differentiation,[44] and iii) angiopoietin-1/Tie-2 paracrine loop reciprocally mediates pericyte−EC interaction and stability.[45] However, the role of the Wnt signaling pathways remain poorly characterized despite evidence that these pathways are crucial for pulmonary angiogenesis. We previously reported that bone morphogenetic protein 2 (BMP2), via BMP receptor 2 (BMPR2), induces β-catenin activation, which is essential for pulmonary artery EC survival and proliferation, whereas the activation of RhoA-Rac1 signaling is necessary for motility.[31] The latter represents the first evidence of Wnt/PCP recruitment in the pulmonary circulation and led us to postulate that this pathway could also be involved in coordinating pericyte motility and polarity.[46] In our model, PAH pericytes had impaired motility and polarity both at baseline and in the presence of PMVECs, and their response to Wnt5a stimulation was significantly less compared to that of control cells, which argues strongly for a defect in the ability of PAH pericytes to activate their Wnt/PCP pathway. Furthermore, given the ability of the Wnt pathways to cross-talk with BMP signaling, it may be of interest to determine whether this interaction is also present in pericytes and whether *BMPR2* mutations can influence Wnt/PCP activation in PAH pericytes.

An important observation was that the ability of pericytes to associate with PMVECs was significantly impaired when both Fzd7 and cdc42 were simultaneously reduced. We speculate that this may be due to the presence of redundant receptors or signaling pathways that compensate when one of these two genes is impaired but fail to do so when both become deficient. Evidence to support our model comes from the fact that there are 10 known Fzd receptors[47] and they are expressed in healthy pericytes in various proportions, thus allowing the possibility that any of these could compensate for Fzd7 loss and preserve Wnt/PCP activation. Furthermore, other pathways known to attract pericytes to blood vessels (eg, PDGF, FGF2) can also target cdc42 independently and may help with its activation when Fzd7 becomes deficient. The small GTPase cdc42 has been shown to be essential for vasculogenesis during embryonic development, and its deletion reduces survival and migration of ECs.[48] However, the fact that pericytes deficient in both Fzd7 and cdc42 lose their ability to interact with ECs in co-culture supports a model in which these two genes work within a vital signaling network that may not be restored by cross-talk with other pathways.

In conclusion, this is the first report of a defect in pericyte motility contributing to the pathobiology of PAH and of a novel role for Wnt/PCP in pericyte recruitment and establishment of endothelial-pericyte contacts. This is relevant as a loss of peripheral pulmonary arteries and impaired regeneration of normal vessels are key pathological features of PAH. As a modifier of BMP signaling in endothelial and smooth muscle cells,[31,49] Wnt/PCP signaling is a strong candidate to understand how pulmonary angiogenesis is orchestrated. Understanding how Wnt/PCP participates in pulmonary angiogenesis will provide a new paradigm to understand how pulmonary vessels can regenerate after injury and should provide new avenues for therapeutic interventions aimed at reversing the progression of PAH.

Acknowledgments

Lung tissues from PAH and control patients were provided by the Pulmonary Hypertension Breakthrough Initiative, which is funded by the Cardiovascular Medical Research And Education Fund. We thank Marlene Rabinovitch and Jeffrey Axelrod for their careful review and thoughtful comments and Vanessa Rojas and Arshi Jha for technical assistance.

Supplemental Data

Supplemental material for this article can be found at *http://dx.doi.org/10.1016/j.ajpath.2014.09.013*.

References

1. Ribatti D, Nico B, Crivellato E: The role of pericytes in angiogenesis. Int J Dev Biol 2011, 55:261−268
2. Yamagishi S, Imaizumi T: Pericyte biology and diseases. Int J Tissue React 2005, 27:125−135
3. Diaz-Flores L, Gutierrez R, Madrid JF, Varela H, Valladares F, Acosta E, Martin-Vasallo P, Diaz-Flores L Jr: Pericytes. Morpho-function, interactions and pathology in a quiescent and activated mesenchymal cell niche. Histol Histopathol 2009, 24:909−969
4. Armulik A, Abramsson A, Betsholtz C: Endothelial/pericyte interactions. Circ Res 2005, 97:512−523
5. Xian X, Hakansson J, Stahlberg A, Lindblom P, Betsholtz C, Gerhardt H, Semb H: Pericytes limit tumor cell metastasis. J Clin Invest 2006, 116:642−651
6. Armulik A, Genove G, Mae M, Nisancioglu MH, Wallgard E, Niaudet C, He L, Norlin J, Lindblom P, Strittmatter K, Johansson BR, Betsholtz C: Pericytes regulate the blood-brain barrier. Nature 2010, 468:557−561
7. Bresnick GH, Davis MD, Myers FL, de Venecia G: Clinicopathologic correlations in diabetic retinopathy. II. Clinical and histologic appearances of retinal capillary microaneurysms. Arch Ophthalmol 1977, 95:1215−1220
8. Barber AJ, Gardner TW, Abcouwer SF: The significance of vascular and neural apoptosis to the pathology of diabetic retinopathy. Invest Ophthalmol Vis Sci 2011, 52:1156−1163
9. Kapanci Y, Ribaux C, Chaponnier C, Gabbiani G: Cytoskeletal features of alveolar myofibroblasts and pericytes in normal human and rat lung. J Histochem Cytochem 1992, 40:1955−1963
10. Teichert-Kuliszewska K, Kutryk MJ, Kuliszewski MA, Karoubi G, Courtman DW, Zucco L, Granton J, Stewart DJ: Bone morphogenetic protein receptor-2 signaling promotes pulmonary arterial endothelial cell survival: implications for loss-of-function mutations in the pathogenesis of pulmonary hypertension. Circ Res 2006, 98:209−217
11. Ricard N, Tu L, Le Hiress M, Huertas A, Phan C, Thuillet R, Sattler C, Fadel E, Seferian A, Montani D, Dorfmuller P, Humbert M, Guignabert C: Increased pericyte coverage mediated by endothelial-derived fibroblast growth factor-2 and interleukin-6 is a source of smooth muscle-like cells in pulmonary hypertension. Circulation 2014, 129:1568−1597
12. Skovseth DK, Kuchler AM, Haraldsen G: The HUVEC/Matrigel assay: an in vivo assay of human angiogenesis suitable for drug validation. Methods Mol Biol 2007, 360:253−268
13. Nayak RC, Berman AB, George KL, Eisenbarth GS, King GL: A monoclonal antibody (3G5)-defined ganglioside antigen is expressed on the cell surface of microvascular pericytes. J Exp Med 1988, 167: 1003−1015
14. Owens GK, Kumar MS, Wamhoff BR: Molecular regulation of vascular smooth muscle cell differentiation in development and disease. Physiol Rev 2004, 84:767−801
15. Arnaoutova I, George J, Kleinman HK, Benton G: The endothelial cell tube formation assay on basement membrane turns 20: state of the science and the art. Angiogenesis 2009, 12:267−274
16. Ladwein M, Rottner K: On the Rho'd: the regulation of membrane protrusions by Rho-GTPases. FEBS Lett 2008, 582:2066−2074
17. Armulik A, Genove G, Betsholtz C: Pericytes: developmental, physiological, and pathological perspectives, problems, and promises. Dev Cell 2011, 21:193−215
18. Goulimari P, Knieling H, Engel U, Grosse R: LARG and mDia1 link Galpha12/13 to cell polarity and microtubule dynamics. Mol Biol Cell 2008, 19:30−40
19. Saunders KB, D'Amore PA: An in vitro model for cell-cell interactions. In Vitro Cell Dev Biol 1992, 28A:521−528
20. Gao B: Wnt regulation of planar cell polarity (PCP). Curr Top Dev Biol 2012, 101:263−295
21. Artus C, Glacial F, Ganeshamoorthy K, Ziegler N, Godet M, Guilbert T, Liebner S, Couraud PO: The Wnt/planar cell polarity signaling pathway contributes to the integrity of tight junctions in brain endothelial cells. J Cereb Blood Flow Metab 2014, 34:433−440
22. Vladar EK, Antic D, Axelrod JD: Planar cell polarity signaling: the developing cell's compass. Cold Spring Harb Perspect Biol 2009, 1: a002964

23. Dijksterhuis JP, Petersen J, Schulte G: WNT/Frizzled signaling: receptor-ligand selectivity with focus on FZD-G protein signaling and its physiological relevance: IUPHAR Review 3. Br J Pharmacol 2014, 171:1195−1209
24. Bentzinger CF, von Maltzahn J, Dumont NA, Stark DA, Wang YX, Nhan K, Frenette J, Cornelison DD, Rudnicki MA: Wnt7a stimulates myogenic stem cell motility and engraftment resulting in improved muscle strength. J Cell Biol 2014, 205:97−111
25. Yu H, Ye X, Guo N, Nathans J: Frizzled 2 and frizzled 7 function redundantly in convergent extension and closure of the ventricular septum and palate: evidence for a network of interacting genes. Development 2012, 139:4383−4394
26. Witzel S, Zimyanin V, Carreira-Barbosa F, Tada M, Heisenberg CP: Wnt11 controls cell contact persistence by local accumulation of Frizzled 7 at the plasma membrane. J Cell Biol 2006, 175:791−802
27. Etienne-Manneville S: Cdc42—the centre of polarity. J Cell Sci 2004, 117:1291−1300
28. Goehring NW, Grill SW: Cell polarity: mechanochemical patterning. Trends Cell Biol 2013, 23:72−80
29. Huang M, Satchell L, Duhadaway JB, Prendergast GC, Laury-Kleintop LD: RhoB links PDGF signaling to cell migration by coordinating activation and localization of Cdc42 and Rac. J Cell Biochem 2011, 112:1572−1584
30. Lee JG, Kay EP: FGF-2-induced wound healing in corneal endothelial cells requires Cdc42 activation and Rho inactivation through the phosphatidylinositol 3-kinase pathway. Invest Ophthalmol Vis Sci 2006, 47:1376−1386
31. de Jesus Perez VA, Alastalo TP, Wu JC, Axelrod JD, Cooke JP, Amieva M, Rabinovitch M: Bone morphogenetic protein 2 induces pulmonary angiogenesis via Wnt-beta-catenin and Wnt-RhoA-Rac1 pathways. J Cell Biol 2009, 184:83−99
32. Weibel ER: On pericytes, particularly their existence on lung capillaries. Microvasc Res 1974, 8:218−235
33. Meyrick B, Reid L: Ultrastructural findings in lung biopsy material from children with congenital heart defects. Am J Pathol 1980, 101: 527−542
34. El-Bizri N, Wang L, Merklinger SL, Guignabert C, Desai T, Urashima T, Sheikh AY, Knutsen RH, Mecham RP, Mishina Y, Rabinovitch M: Smooth muscle protein 22alpha-mediated patchy deletion of Bmpr1a impairs cardiac contractility but protects against pulmonary vascular remodeling. Circ Res 2008, 102:380−388
35. Bryan BA, D'Amore PA: Pericyte isolation and use in endothelial/pericyte coculture models. Methods Enzymol 2008, 443:315−331
36. Koh W, Stratman AN, Sacharidou A, Davis GE: In vitro three dimensional collagen matrix models of endothelial lumen formation during vasculogenesis and angiogenesis. Methods Enzymol 2008, 443: 83−101
37. Valarmathi MT, Davis JM, Yost MJ, Goodwin RL, Potts JD: A 3D model of vasculogenesis. Biomaterials 2009, 30:1098−1112
38. Singh RK, Seliktar D, Putnam AJ: Capillary morphogenesis in PEG-collagen hydrogels. Biomaterials 2013, 34:9331−9340
39. Nakatsu MN, Sainson RC, Aoto JN, Taylor KL, Aitkenhead M, Perez-del-Pulgar S, Carpenter PM, Hughes CC: Angiogenic sprouting and capillary lumen formation modeled by human umbilical vein endothelial cells (HUVEC) in fibrin gels: the role of fibroblasts and Angiopoietin-1. Microvasc Res 2003, 66:102−112
40. Tuder RM, Voelkel NF: Angiogenesis and pulmonary hypertension: a unique process in a unique disease. Antioxid Redox Signal 2002, 4: 833−843
41. Tuder RM, Cool CD, Yeager M, Taraseviciene-Stewart L, Bull TM, Voelkel NF: The pathobiology of pulmonary hypertension. Endothelium. Clin Chest Med 2001, 22:405−418
42. Petrie RJ, Doyle AD, Yamada KM: Random versus directionally persistent cell migration. Nat Rev Mol Cell Biol 2009, 10:538−549
43. Soriano P: Abnormal kidney development and hematological disorders in PDGF beta-receptor mutant mice. Genes Dev 1994, 8:1888−1896
44. Li DY, Sorensen LK, Brooke BS, Urness LD, Davis EC, Taylor DG, Boak BB, Wendel DP: Defective angiogenesis in mice lacking endoglin. Science 1999, 284:1534−1537
45. Sundberg C, Kowanetz M, Brown LF, Detmar M, Dvorak HF: Stable expression of angiopoietin-1 and other markers by cultured pericytes: phenotypic similarities to a subpopulation of cells in maturing vessels during later stages of angiogenesis in vivo. Lab Invest 2002, 82: 387−401
46. Fenstermaker AG, Prasad AA, Bechara A, Adolfs Y, Tissir F, Goffinet A, Zou Y, Pasterkamp RJ: Wnt/planar cell polarity signaling controls the anterior-posterior organization of monoaminergic axons in the brainstem. J Neurosci 2010, 30:16053−16064
47. MacDonald BT, He X: Frizzled and LRP5/6 receptors for Wnt/β-catenin signaling. Cold Spring Harb Perspect Biol 2012, 4
48. Jin Y, Liu Y, Lin Q, Li J, Druso JE, Antonyak MA, Meininger CJ, Zhang SL, Dostal DE, Guan JL, Cerione RA, Peng X: Deletion of Cdc42 enhances ADAM17-mediated vascular endothelial growth factor receptor 2 shedding and impairs vascular endothelial cell survival and vasculogenesis. Mol Cell Biol 2013, 33:4181−4197
49. Perez VA, Ali Z, Alastalo TP, Ikeno F, Sawada H, Lai YJ, Kleisli T, Spiekerkoetter E, Qu X, Rubinos LH, Ashley E, Amieva M, Dedhar S, Rabinovitch M: BMP promotes motility and represses growth of smooth muscle cells by activation of tandem Wnt pathways. J Cell Biol 2011, 192:171−188